J Supercond Nov Magn (2017) 30:395–399
DOI 10.1007/s10948-016-3745-2

ORIGINAL PAPER

Characterization of Nano-Particle $Co_{1-x}Zn_xFe_2O_4$ Synthesized Using Alove Vera Gel

Manoj M. Kothawale[1] · Rajesh Pednekar[2] · U. B. Gawas[2] · S. S. Meena[3] · N. Prasad[4] · Santhosh Kumar[4]

Received: 18 July 2016 / Accepted: 19 August 2016 / Published online: 31 August 2016

Abstract Nano-particle $Co_{1-x}Zn_xFe_2O_4$ (x = 0.0, 0.3, 0.5, 0.7, and 1.0) samples were prepared via combustion route using Alove Vera Gel. XRD, IR, and SAED analysis represents single-phase formation of ferrite samples, and nano-sizes of the particles in the range of 6 to 13 nm were confirmed using XRD data and TEM images. Decrease in lattice constant with increasing Zn content reflects formation of compositionally homogeneous samples. Dielectric constant and dielectric loss study showed promising results. The room temperature Mossbauer spectrum showed mixed superparamagnetic and ordered ferromagnetic behavior. The possible modification in the cation distributions was seen in the nano-particle $ZnFe_2O_4$ sample obtained in the present work compared to conventional bulk samples.

Keywords Co–Zn ferrites · XRD · TEM · Dielectric constant · Mossbauer spectra

✉ Manoj M. Kothawale
manojkothawale@yahoo.com

[1] Department of Physics, D.M.'S College and Research Centre, Assagao, Goa 403 507, India

[2] Department of Chemistry, D.M.'S College and Research Centre, Assagao, Goa 403 507, India

[3] Solid State Physics Division, Physics Division, Bhabha Atomic Research Centre, Mumbai 400085, India

[4] Department of Metallurgical Engineering, Indian Institute of Technology (Banaras Hindu University), Varanasi 221005, India

1 Introduction

Ferrites are the mixed metal oxide materials which find wide applications as electric, magnetic, and catalytic materials. Spinel structure ferrites represent a class of magnetic materials which are of technological importance [1, 2]. They are used in electronic industry for manufacturing conventional antenna rods, intermediate frequency transformer cores for switching powers, fly back transformer cores, filter cores used in television sets, communication devices, etc. Cobalt-zinc ferrites is known to be used for applications including magnetic cell separation, switch devices, magnetic cores in power supplies, permanent magnets, flexible recording media, hard disc recording media, etc. Advanced research of using nano-particles ferrites for drug delivery systems in cancer therapy is being largely carried out across the globe. A number of solution-based preparation techniques are available for the preparation of nano-particle ferrites. In spite of this, obtaining ferrite nanoparticles with desirable size and magnetic properties is still a challenge. The properties are found to be dependent on the method of synthesis. Here, we have reported synthesis of $Co_{1-x}Zn_xFe_2O_4$ nanoparticles by modified combustion route using plant extract, their characterizations, Mossbauer studies, and dielectric measurements.

2 Experimental

Calculated amount of raw materials namely cobalt nitrate, zinc nitrate, and ferric nitrate (all salts of AR grade) were dissolved in 100 ml of distilled water in a flask separately. Ten milliliters of each of these solutions was added to a beaker containing pre-calculated Alove Vera Gel. The

mixture was then kept on a hot plate and stirred constantly around 1 h. The brown gel-like residue was obtained. The residue was incinerated in a silica crucible. Ultrafine ferrite powder was obtained which is highly magnetic. The X-ray powder diffraction patterns were recorded on a Rigaku X-ray diffractometer using CuKα radiation and 2θ scanning range from 20° to 80°. IR spectra for all the samples were recorded using Shimatzu Fourier transform infrared (FTIR) 8900 spectrometer in the range of range of 300 to 1000 cm^{-1}. Samples were prepared in the form of pallets with KBr to specimen ratio as 1:100 for IR measurements. Transmission electron microscope (TEM) images were recorded on (TEM, TECHNAI G^2) with an acceleration voltage 200 kV. The room temperature Mössbauer spectrum of the sample was recorded in constant acceleration mode using a ^{57}Co Mössbauer source. The calibration of the velocity scale was done using ^{57}Fe metal foils. Dielectric measurements were recorded at room temperature within a frequency range from 100 Hz to 10 MHz using Wayne Kerr 6500P precision component analyzer setup.

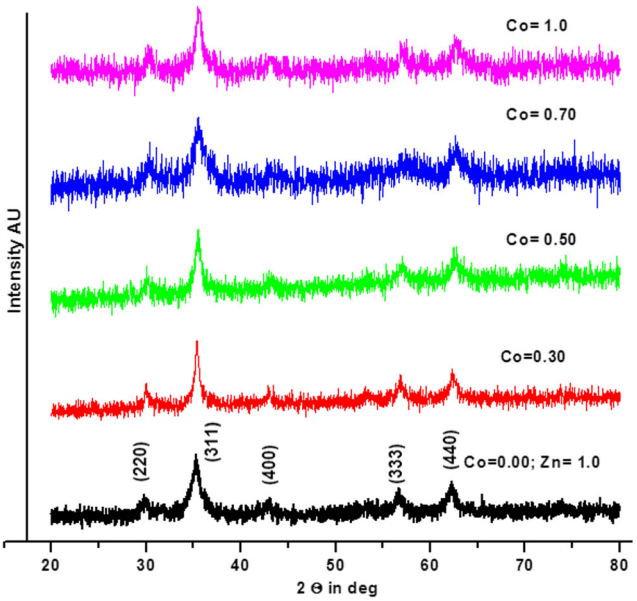

Fig. 1 XRD patterns for $Co_{1-x}Zn_xFe_2O_4$ ($x = 0.0$, 0.3, 0.5, 0.7, and 1.0) samples

3 Results and Discussion

3.1 XRD Analysis

The X-ray diffraction (XRD) patterns of the $Co_{1-x}Zn_xFe_2O_4$ ($x = 0.0$, 0.3, 0.5, 0.7, and 1.0) samples are shown in Fig. 1. The X-ray diffraction pattern shows all the peak characteristics of the cubic spinel ferrites with no secondary phases. This confirms the formation of single phase ferrite samples. The crystallite sizes of samples using (3 1 1) plane were calculated by Debye–Scherrer formula and are given in Table 1. The sizes were found to be in the range of 6 to 13 nm. The lattice parameters (a) decreases with increase in zinc concentration. The decrease in a can be explained on the basis of the ionic radii of Co^{+2} and Zn^{+2} (Co^{+2} as 0.67 Å and Zn^{+2} as 0.74 Å).

3.2 TEM Analysis

The TEM image and histogram depicting particle size distribution for the sample with Zn = 0.7 is shown in Fig. 2. Typical morphologies visualized by TEM image show that in all cases, the prepared particles are nano-sized largely spherical in shape and have low agglomeration. The histogram curve show maxima in the range of 6 to 8 nm and is in good agreement with crystallite sizes of 6 nm obtained from XRD analysis. The corresponding selected area electron diffraction (SAED) pattern of the sample shows spotty ring pattern without any additional diffraction spots and rings of second phases, revealing their crystalline spinel structure. Measured interplanar spacings (d_{hkl}) from SAED pattern are in good agreement with the XRD results. The diffraction rings are identified as the (111), (200), (220), (311), and (222).

3.3 IR Analysis

The IR absorption spectra of all the samples show two absorption bands as shown in Fig. 3. The higher band ν_1 is between wave number 600 and 550 cm^{-1} which corresponds to intrinsic stretching vibrations of metals at the tetrahedral site whereas lower band ν_2 between 450 and 385 cm^{-1} is assigned to octahedral metal stretching. This is a common feature of all the ferrites indicating single phase spinal structure having two sub-lattices [3].

Table 1 Lattice constant (a) and crystallite size (D) of $Co_{1-x}Zn_xFe_2O_4$ ($x = 0$, 0.30, 0.5, 0.7, and 1.0) derived from XRD spectrum

Sample Zn = x	a (Å)	D(311) (nm)
0	8.4384	8.85
0.3	8.4185	13.14
0.5	8.3867	13.26
0.7	8.3847	6.09
0.1	8.3841	12.0

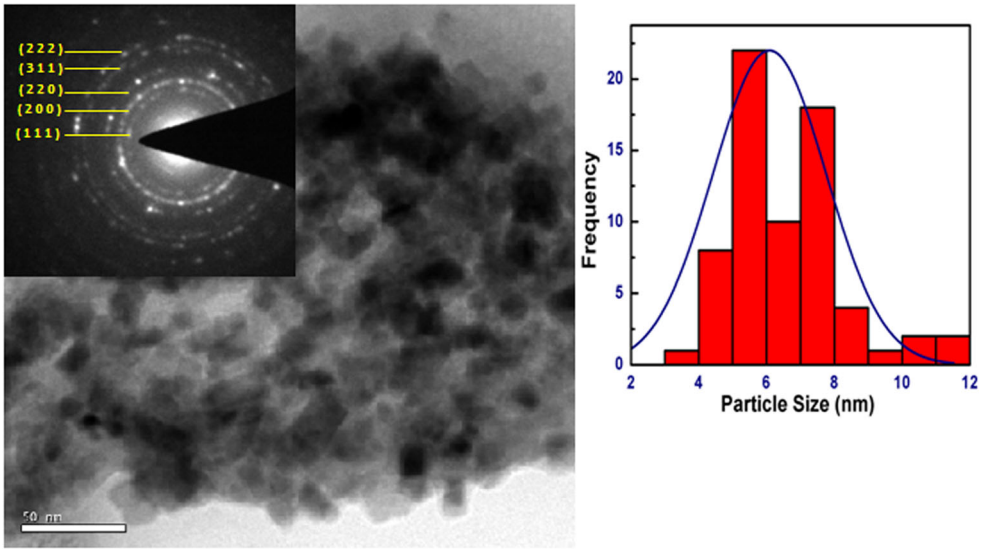

Fig. 2 TEM image with SAED for $Co_{0.3}Zn_{0.7}Fe_2O_4$ sample and corresponding histogram of particle size distribution

3.4 Dielectric Analysis

The frequency variation of dielectric constant of $Co_{1-x}Zn_xFe_2O_4$ ($x = 0.0$, 0.3, 0.5, 0.7, and 1.0) ferrite samples at room temperature in the frequency range of 20 Hz to 10 MHz is presented in Fig. 4. The dielectric constant shows sharp decrease up to 1 KHz, followed by a gradual decrease from 1 to 10 KHz and is nearly independent of frequency from 10 KHz to 10 MHz. The dielectric constant of any material, in general, is due to dipolar, electronic, ionic, and interfacial polarization. In the lower-frequency region, surface polarization contributes predominantly then electronic or ionic polarization in determining the dielectric properties of ferrite materials. The decrease in dielectric constant with increasing frequency is a normal behavior observed in most of ferromagnetic materials. The high value of dielectric constant observed at lower frequencies is explained on the basis of space charge polarization due to in-homogeneous dielectric structure

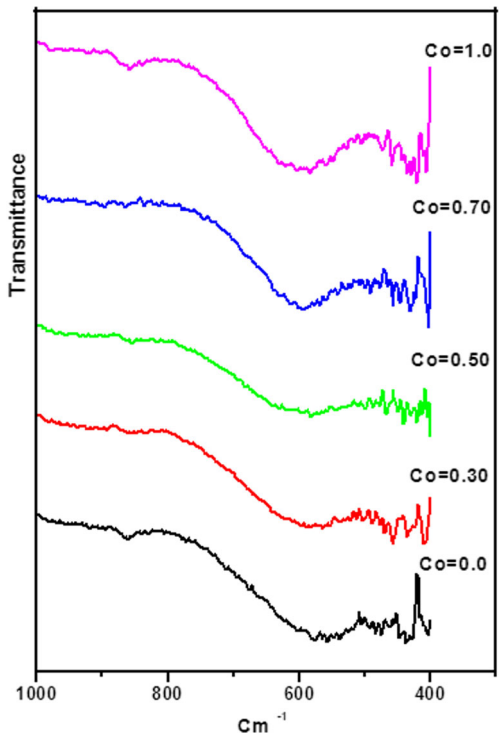

Fig. 3 IR spectrum of $Co_{1-x}Zn_xFe_2O_4$ ($x = 0.0$, 0.3, 0.5, 0.7, and 1.0) samples

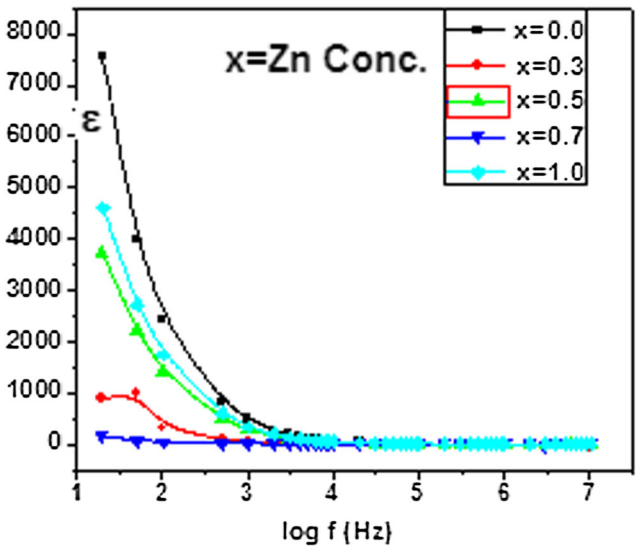

Fig. 4 Variation of dielectric constant versus frequency for $Co_{1-x}Zn_xFe_2O_4$ ($x = 0.0$, 0.3, 0.5, 0.7, and 1.0) samples

[4, 5]. The variation of dielectric loss with frequency at room temperature is depicted in the Fig. 5. The dielectric loss gives the loss of energy from the applied field into the sample. The dielectric loss in ferrite materials depends on a number of factors such as stoichiometry, Fe^{+2} concentration and structural homogeneity which in turn depend on the composition and method of preparation. The dielectric losses of $Co_{1-x}Zn_xFe_2O_4$ ferrite samples in present work were found to be very low (0.10 to 2) in the higher-frequency (100 KHz to 1 MHz) region.

3.5 Mössbauer Spectroscopy

Figure 6 shows room temperature Mössbauer spectra of samples and corresponding hyperfine parameters are listed in Table 2. Mossbauer spectra of $CoFe_2O_4$ exhibit two normal zeeman split sextets due to the A-site Fe^{3+} ions and other due to B-site Fe^{3+} having hyperfine fields 47.7 and 42.9 T, respectively, which indicates ferrimagnetic behavior of the sample. In case of $Co_{0.5}Zn_{0.5}Fe_2O_4$ show central doublet with population of 15.6 % superimposed on a broad magnetic sextets, indicating the partial transformation to an ordered magnetic structure. The doublet can be assigned to superparamagnetic nanoparticles. This presence of both superparamagnetic and ferrimagnetic particles may be due to the wide size distribution or effect of preparation. The $ZnFe_2O_4$ sample shows quadrupole doublet with IS = 0.351 mm/s, QS = 0.475 mm/s, indicating paramagnetic nature. Spectrum also contains one sextet covering 12.5 % area. In bulk form, $ZnFe_2O_4$ is a normal spinel with Zn^{2+} ions located in the A-sites and Fe^{3+} ions in the B-sites; it behaves as an antiferromagnet below 10 K and a paramagnet above this temperature. Superimposition of magnetically split sextet on quadrupole doublet may be due to the presence of both ferrimagnetic and superparamagnetic particles. At nano-range particles, some percentage of Fe^{3+} ions might have pushed to the tetrahedral sites which switches on the A–B super-exchange interaction between Fe^{3+} ions on both the sites and gives rise to ferrimagnetic ordering. Thus, redistribution of cations in the

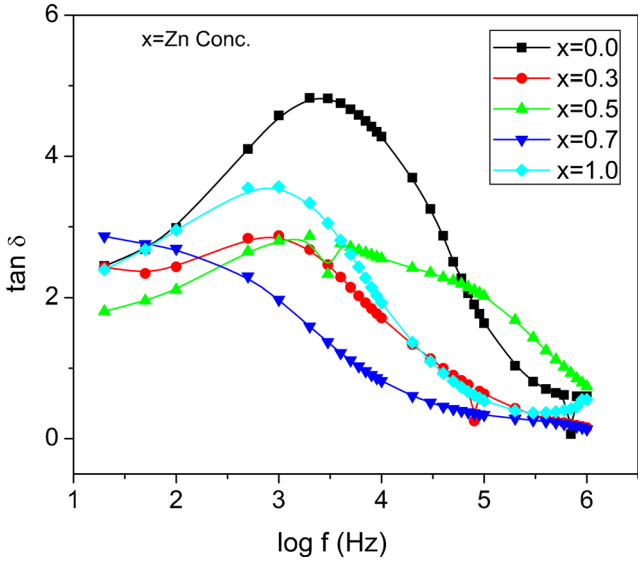

Fig. 5 Variation of dielectric loss versus frequency for $Co_{1-x}Zn_xFe_2O_4$ ($x = 0.0$, 0.3, 0.5, 0.7, and 1.0) samples

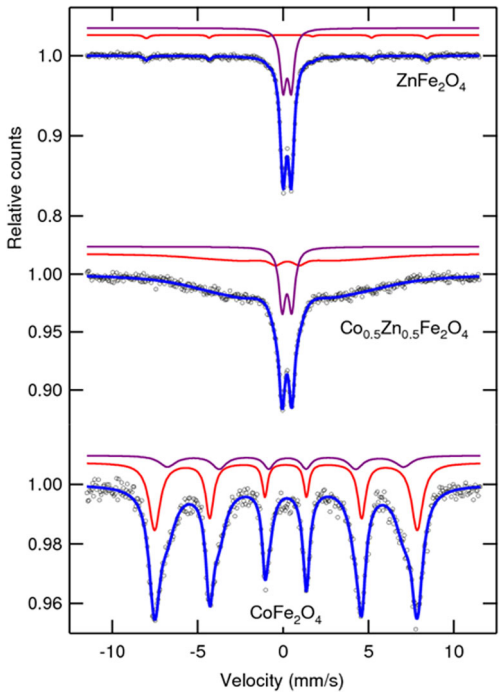

Fig. 6 Room temperature Mössbauer spectrum for the samples

Table 2 The isomer shift (δ), quadrupole splitting (ΔE_Q), hyperfine Field values (H_{hf}), and areas in percentage of $Co_{1-x}Zn_xFe_2O_4$ ($x = 0$, 0.5 and 1.0) derived from Mössbauer spectra recorded at room temperature

Sample	Isomer shift[a] (δ) mm/s	Quadru. splitting (ΔE_Q) mm/s	Hyperfine field (H_{hf}) T	Area (%)
$X = 0$				
Sextet 1	0.271	−0.011	47.7	59.5
Sextet 2	0.310	0.011	42.9	40.5
$X = 0.5$				
Doublet	0.340	0.556	–	15.6
Sextet	0.407	0.079	27.2	84.4
$X = 1.0$				
Doublet	0.351	0.475	–	87.5
Sextet	0.428	−0.221	50.6	12.5

[a]Isomer shift values are relative to α-Fe (0.00 mm/s) foil

nanocrystalline $ZnFe_2O_4$ compared to bulk form is possible [6, 7].

4 Conclusions

Nano-particles of cobalt zinc ferrite were successfully prepared by modified combustion method using Aloe Vera Gel. Characterizations of the samples were carried out using XRD, TEM, FTIR, and Mossbauer spectroscopy techniques. Crystallite sizes calculated using XRD data is in good agreement with particle sizes obtained from TEM results. Low dielectric losses at higher frequency were observed in the samples. Cluster of superparamagnetic particles were observed in the room temperature Mossbauer spectroscopy analysis. Low-temperature Mossbauer studies can be undertaken in the future to understand magnetic structure in further detail along with temperature dependence dielectric studies.

References

1. Cavicchi, R.E., Silsbe, R.H.: Phys. Rev. Lett. **52**(16), 1453–1456 (1984)
2. Shinde, A.B.: International Journal of Innovative Technology and Exploring Engineering **3**(4) (2013)
3. Ladgaonkar, B.P., Kolekar, C.B., Vaingankar, A.S.: Bull. Mater. Sci. **25**, 351–358 (2002)
4. Waldron, R.D.: Phys. Rev. B **99**(6), 1727 (1955)
5. Verma, A., Goel, T.C., Mendiratta, R.G., Gupta, R.G.: J. Magn. Magn. Mater. **192**, 271 (1999)
6. Arulmurugana, R., Vaidyanathana, G., Sendhilnathanb, S., Jeyadevan, B.: Physica B **363**, 225–231 (2005)
7. Chinnasamy, C.N., Narayanasamy, A., Ponpandian, N., Chattopadhyay, K., Guerault, H., Greneche, J.M.: J. Phys. Condens. Matter **12**, 7795–7805 (2000)